frontiers in Physics

ORIGINAL RESEARCH
published: 30 September 2021
doi: 10.3389/fphy.2021.752137

Optical Frequency Down-Conversion With Bandwidth Compression Based on Counter-Propagating Phase Matching

Dong-Jie Guo, Ran Yang, Yi-Chen Liu, Jia-Chen Duan, Zhenda Xie, Yan-Xiao Gong* and Shi-Ning Zhu*

National Laboratory of Solid State Microstructure, School of Physics, School of Electronic Science and Engineering, and Collaborative Innovation Center of Advanced Microstructures, Nanjing University, Nanjing, China

Optical quantum network plays an important role in large scale quantum communication. However, different components for photon generation, transmission, storage and manipulation in network usually cannot interact directly due to the wavelength and bandwidth differences, and thus interfaces are needed to overcome such problems. We propose an optical interface for frequency down-conversion and bandwidth compression based on the counter-propagating quasi-phase-matching difference frequency generation process in the periodically-poled lithium niobate on insulator waveguide. We prove that a separable spectral transfer function can be obtained only by choosing proper pump bandwidth, thus relaxing the limitation of material, dispersion, and working wavelength as a result of the counter-propagation phase-matching configuration. With numerical simulations, we show that our design results in a nearly separable transfer function with the Schmidt number very close to 1. With proper pump bandwidth, an photon at central wavelength of 550 nm with a bandwidth ranging from 50 GHz to 5 THz can be converted to a photon at central wavelength of 1,545 nm with a much narrower bandwidth of 33 GHz.

Keywords: frequency conversion, bandwidth compression, counter-propagating quasi-phase-matching, periodically-poled lithium niobate on insulator waveguide, difference frequency generation

OPEN ACCESS

Edited by:
Bao-Sen Shi,
University of Science and Technology of China, China

Reviewed by:
Qiang Zhang,
University of Science and Technology of China, China
Yunfeng Huang,
University of Science and Technology of China, China

****Correspondence:***
Zhenda Xie
xiezhenda@nju.edu.cn
Yan-Xiao Gong
gongyanxiao@nju.edu.cn

Specialty section:
This article was submitted to Optics and Photonics, a section of the journal Frontiers in Physics

Received: *02 August 2021*
Accepted: *15 September 2021*
Published: *30 September 2021*

Citation:
Guo D-J, Yang R, Liu Y-C, Duan J-C, Xie Z, Gong Y-X and Zhu S-N (2021) Optical Frequency Down-Conversion With Bandwidth Compression Based on Counter-Propagating Phase Matching. Front. Phys. 9:752137. doi: 10.3389/fphy.2021.752137

1 INTRODUCTION

Photons play an important role in quantum information science, such as long distance quantum communication [1,2], linear optical quantum computation [3,4] and interface to quantum memories [5,6]. However, in these applications, different devices and systems usually require different photon central frequencies and bandwidths. In order to combine all these systems in one quantum network, photon frequency interface capable of converting frequency and bandwidth is indispensable.

Electro-optical modulation is an efficient way to shift photon frequency [7–9], which is commonly used in pulse manipulation, however, its conversion range is limited to several GHz. Sum frequency generation (SFG) [10–12] and difference-frequency generation (DFG) [13] in nonlinear optical process are beneficial to frequency conversion between different frequency bands and have been utilized as an interface between the visible and communication wavelength bands [14–16]. Moreover, a bandwidth compression factor of 40 was achieved by utilizing SFG process with chirped input photon and anti-chirped strong pump laser [17]. However, interfaces generated by this way usually

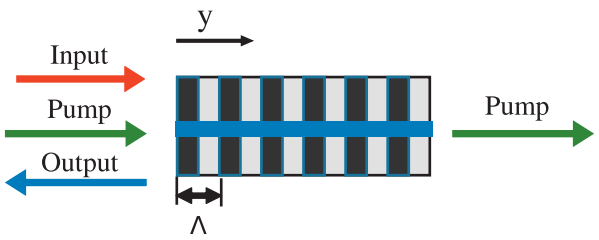

FIGURE 1 | Geometry of a counter-propagating quasi-phase-matching difference frequency generation process in a y-direction waveguide with a poling period of Λ. The input and pump light propagate in the same direction, while the output light propagates in the opposite direction.

suffer from low conversion efficiency due to the need of ultra wide phase-matching bandwidth. How to convert frequency and compress bandwidth effectively at the same time is a big challenge. Recently, Allgaier *et al.* made an approach towards both goals with dispersion-engineered SFG [18], where photon at communication wavelength was converted to the visible range with a bandwidth compression factor of 7.47 and an internal conversion efficiency of 61.5%. Such method relies on modulating the dispersion and group velocity relationship among the input, pump, and output photons, and thus has limited choices on the working wavelengths and materials.

On the other hand, counter-propagating quasi-phase-matching (QPM) spontaneous parametric down-conversion (SPDC) process has been extensively studied due to its unique spectral properties [19,20], such as narrow bandwidth [21,22] and frequency uncorrelated [23–26] photon pairs. In contrast to the traditional co-propagating process, in the counter-propagating process the phase-matching function is greatly affected by the counter propagation of the signal and idler photons, and hence such method can be applied in a large range of nonlinear materials and working wavelengths. In this paper, we propose to use the counter-propagating QPM DFG to realize an optical interface for frequency down-conversion and bandwidth compression. We design an experimental feasible waveguide structure based on the thin-film lithium niobate on insulator (LNOI) platform, which has been considered as a revolutionary platform for integrated photonics [27] and aroused a great deal of interest in recent years, as it allows a strong optical confinement and thus brings strong nonlinear effects [28–30].

2 METHODS

The configuration of a counter-propagating QPM DFG process is shown in **Figure 1**. With a pulse laser as the pump in a *y*-direction waveguide, a co-propagating high-frequency input photon is converted into a low-frequency output photon in the counter-propagation direction. In the undepleted pump approximation, the effective Hamiltonian describing the DFG process can be written as [31].

$$H = \int dt\hat{H}(t) = \theta \iint d\omega_i d\omega_o f(\omega_i, \omega_o)\hat{a}_i(\omega_i)\hat{a}_o^{\dagger}(\omega_o) + H.c., \quad (1)$$

where θ is the coupling parameter having absorbed all the constants, and the frequencies are constrained by the energy-conservation relation of $\omega_i - \omega_p = \omega_o$, with the subscripts i, p, and o representing the input, pump, and output photons, respectively. The normalized DFG transfer function can be expressed as $f(\omega_i, \omega_o) = \alpha(\omega_i - \omega_o)\Phi(\omega_i, \omega_o)$, where $\alpha(\omega_i - \omega_o)$ is the spectral amplitude of pump light and $\Phi(\omega_i, \omega_o)$ denotes the phase matching function.

With broadband pump laser, the transfer function can be written as Schmidt decomposition form [32].

$$f(\omega_i, \omega_o) = \sum_{j=1}^{K} \kappa_j \phi_j(\omega_i)\psi_j(\omega_o), \quad (2)$$

where $\{\phi_j(\omega_i)\}$ and $\{\psi_j(\omega_o)\}$ are two sets of orthogonal spectral amplitude functions and κ_j are the real Schmidt coefficients satisfying $\sum_j \kappa_j^2 = 1$. Thus the effective Hamiltonian can be rewritten as

$$H = \theta \sum_j \kappa_j A_j C_j^{\dagger} + H.c., \quad (3)$$

with broadband mode operators $A_j = \int d\omega \phi_j(\omega)\hat{a}_i(\omega)$ and $C_j = \int d\omega \psi_j(\omega)\hat{a}_o(\omega)$. Compared with the effective Hamiltonian of an optical beam splitter (BS) $H_{BS} = \theta \hat{a}\hat{c}^{\dagger} + H.c.$[33], the DFG process can be considered as a set of independent BSs which convert A_j to C_j with effective coupling parameter $\theta\kappa_j$, namely, $A_j \rightarrow \cos(\theta\kappa_j)A_j + i\sin(\theta\kappa_j)C_j$ with conversion efficiency $\sin^2(\theta\kappa_j)$ [31]. Hence, for the multi-mode input photon $\sum_j \alpha_j A_j^{\dagger}|0\rangle$, with $\sum \alpha_j^2 = 1$, the total conversion efficiency is given by $\sum_j |\alpha_j|^2 \sin^2(\theta\kappa_j)$. We can see that, given a fixed pump light power, the maximum total conversion efficiency is achieved when the Schmidt number $K = 1$, i.e., the transfer function is separable, according to the Cauchy-Schwarz inequality. Hence, it is important to design a separable transfer function for efficient frequency conversion. In the following, we propose a method to obtain a separable transfer function by using the counter-propagating QPM DFG process.

The phase matching function can be expressed as

$$\Phi(\omega_i, \omega_o) = \mathrm{sinc}\left(\frac{\Delta kL}{2}\right)e^{i\frac{\Delta kL}{2}}, \quad (4)$$

with L denoting the poling length. For the counter-propagating DFG process, the phase mismatch Δk is given by

$$\Delta k = k_i - k_p + k_o - k_G, \quad (5)$$

where $k_G = 2\pi m/\Lambda$ is the mth order reciprocal wave vector with Λ denoting the poling period.

We define frequency offsets $\Delta\omega_j \equiv \Omega_j - \omega_j$, with $j = i, p, o$, where Ω_j are central frequencies satisfying perfect phase-matching condition $\Delta k = 0$. Thus, according to the energy-conservation relation, we have $\Omega_i - \Omega_p = \Omega_o$, and $\Delta\omega_i - \Delta\omega_p = \Delta\omega_o$. Then, by expanding Δk to the first order in $\Delta\omega_j$ and $\Delta\omega_o$ around central frequencies, we obtain

$$\Delta k = \left(u_i^{-1} - u_p^{-1}\right)\Delta\omega_i + \left(u_o^{-1} + u_p^{-1}\right)\Delta\omega_o, \quad (6)$$

where $u_j, j = i, o, p$ are the group velocities at central frequencies. For comparison, the phase mismatch of the co-propagating DFG process given by $\Delta k_{co} = k_i - k_p - k_o - k_G$, can be expanded as

$$\Delta k_{co} = \left(u_i^{-1} - u_p^{-1}\right)\Delta\omega_i + \left(u_p^{-1} - u_o^{-1}\right)\Delta\omega_o. \tag{7}$$

We can see that in the traditional co-propagating process the coefficients of frequency offsets only depend on the difference of the reciprocal of group velocities, and thus in such process the phase-matching function is usually engineered by selecting working frequencies and structures to control the dispersion and group velocities [34]. While, in the counter-propagating process, the coefficients also depend on the sum of the group velocities, enabling intrinsic features for phase-matching engineering [20–26].

To further characterize the transfer function, we define two characteristic bandwidth scales

$$\delta\omega_1 = \frac{2}{\left(u_i^{-1} - u_p^{-1}\right)L}, \qquad \delta\omega_2 = \frac{2}{\left(u_o^{-1} + u_p^{-1}\right)L}. \tag{8}$$

Thus, the phase matching function given by **Eq. 4** can be rewritten as

$$\tilde{\Phi}\left(\frac{\Delta\omega_i}{\delta\omega_1} + \frac{\Delta\omega_o}{\delta\omega_2}\right) = \mathrm{sinc}\left(\frac{\Delta\omega_i}{\delta\omega_1} + \frac{\Delta\omega_o}{\delta\omega_2}\right)e^{-i\left(\frac{\Delta\omega_i}{\delta\omega_1} + \frac{\Delta\omega_o}{\delta\omega_2}\right)}, \tag{9}$$

where we defined a function of $\tilde{\Phi}(x) \equiv \mathrm{sinc}(x)e^{-ix}$. By rewriting the pump amplitude function $\alpha(\omega_i - \omega_o)$ as $\tilde{\alpha}(\Delta\omega_i - \Delta\omega_o)$, we can write the transfer function against frequency offsets as

$$\tilde{f}(\Delta\omega_i, \Delta\omega_o) = \tilde{\alpha}(\Delta\omega_i - \Delta\omega_o)\tilde{\Phi}\left(\frac{\Delta\omega_i}{\delta\omega_1} + \frac{\Delta\omega_o}{\delta\omega_2}\right) \tag{10}$$

In the following, we prove that when the pump light bandwidth $\delta\omega_p$ satisfies $\delta\omega_2 \ll \delta\omega_p \ll \delta\omega_1$, the transfer function can approach a separable function of $\Delta\omega_i$, $\Delta\omega_o$. In analogy to the analysis in Ref. [20], we first recast the argument of function $\tilde{\Phi}$

$$\frac{\Delta\omega_i}{\delta\omega_1} + \frac{\Delta\omega_o}{\delta\omega_2} = \frac{\Delta\omega_p}{\delta\omega_1} + \left(\frac{\Delta\omega_o}{\delta\omega_1} + \frac{\Delta\omega_o}{\delta\omega_2}\right) \approx \frac{\Delta\omega_o}{\delta\omega_3}, \tag{11}$$

with

$$\delta\omega_3 = \frac{2}{\left(u_i^{-1} + u_o^{-1}\right)L}, \tag{12}$$

where $\Delta\omega_p/\delta\omega_1$ has been neglected because it is on the order $\delta\omega_p/\delta\omega_1 \ll 1$. Then we recast the argument of function $\tilde{\alpha}$ as

$$\Delta\omega_i - \Delta\omega_o = \Delta\omega_i\left(1 + \frac{\delta\omega_2}{\delta\omega_1}\right) - \delta\omega_2\left(\frac{\Delta\omega_i}{\delta\omega_1} + \frac{\Delta\omega_o}{\delta\omega_2}\right). \tag{13}$$

where $\Delta\omega_i/\delta\omega_1 + \Delta\omega_o/\delta\omega_2$ is the argument of the sinc function in $\tilde{\Phi}$ as given in **Eq. 9**, and thus it is limited to values on the order of ~ 10, namely, inside the bandwidth of sinc function, due to the product relationship of $\tilde{\alpha}$ and $\tilde{\Phi}$ shown in **Eq. 10**. Consequently, provided that $\delta\omega_2/\delta\omega_p$ is small enough, we can have $\delta\omega_2\left(\Delta\omega_i/\delta\omega_1 + \Delta\omega_o/\delta\omega_2\right)$ much smaller than $\delta\omega_p$, the bandwidth of $\tilde{\alpha}$, and

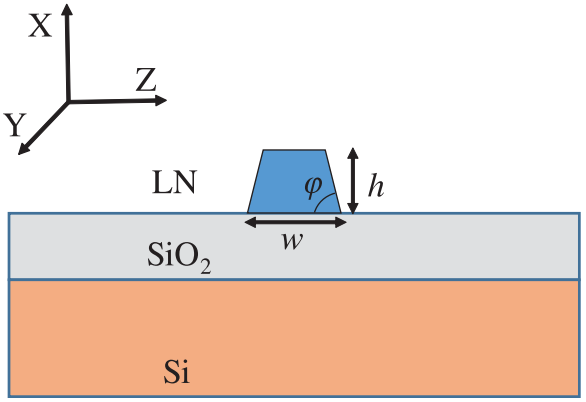

FIGURE 2 | Schematic of the X-cut LNOI waveguide structure. The parameters φ, w, and h denote sidewall angle, bottom ridge width, and hight of the waveguide, respectively.

therefore this term is negligible in the argument of $\tilde{\alpha}$. Hence we have the following approximation

$$\tilde{\alpha}(\Delta\omega_i - \Delta\omega_o) \approx \tilde{\alpha}\left[\Delta\omega_i\left(1 + \frac{\delta\omega_2}{\delta\omega_1}\right)\right]. \tag{14}$$

In addition, considering $\delta\omega_2/\delta\omega_1 \ll 1$, we can further make approximation on **Eq. 14** as

$$\tilde{\alpha}(\Delta\omega_i - \Delta\omega_o) \approx \tilde{\alpha}(\Delta\omega_i). \tag{15}$$

Consequently, the transfer function given by **Eq. 10** approaches the factorized form

$$\tilde{f}(\Delta\omega_i, \Delta\omega_o) \approx \tilde{\alpha}(\Delta\omega_i)\tilde{\Phi}\left(\frac{\Delta\omega_o}{\delta\omega_3}\right). \tag{16}$$

Such separable function also means that the correlation between the input and output photons is eliminated. It is clear that the frequency of the input photon can vary within the bandwidth of the pump light, and thus the bandwidth of the input photon can be as large as that of the pump light, namely, $\delta\omega_i = \delta\omega_p$. While, the bandwidth of the output photon is only determined by the phase-matching function irrespective of the pump bandwidth, which can be obtained from the full width at half maximum of the spectral density function $|\tilde{\Phi}\left(\Delta\omega_o/\delta\omega_3\right)|^2 = |\mathrm{sinc}\left(\Delta\omega_o/\delta\omega_3\right)|^2$, given by

$$\delta\omega_o = 2.78\delta\omega_3 = \frac{5.56}{\left(u_i^{-1} + u_o^{-1}\right)L}. \tag{17}$$

Hence, we can get the bandwidth compression factor as

$$\eta = \frac{\delta\omega_i}{\delta\omega_o} = \frac{1}{5.56}\delta\omega_p L\left(u_i^{-1} + u_o^{-1}\right). \tag{18}$$

3 RESULTS

The schematic of the LNOI waveguide is shown in **Figure 2** consisting of three layers of silicon (Si), silica (SiO_2), and lithium

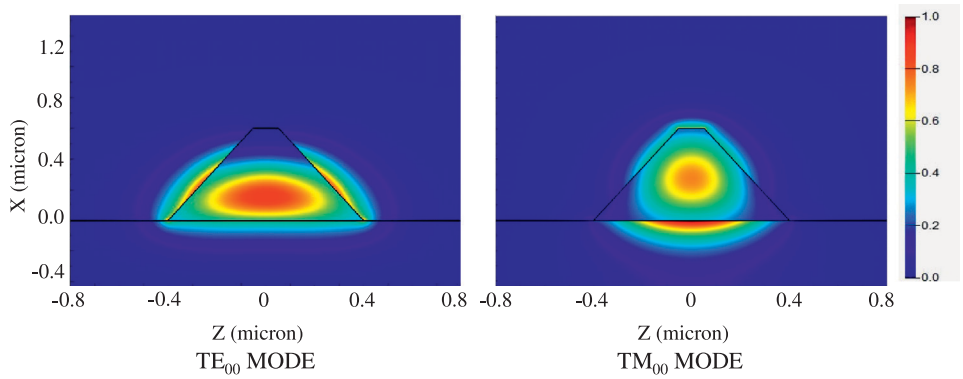

FIGURE 3 | Field distribution of TM_{00} mode and TE_{00} mode at 1,545 nm.

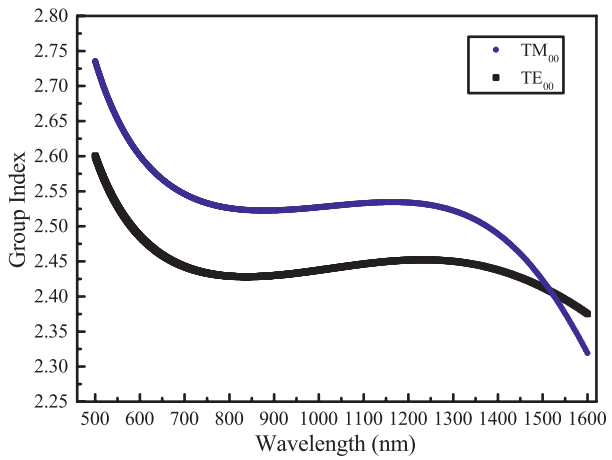

FIGURE 4 | Group index of TE_{00} and TM_{00} modes in LNOI waveguide with wavelength ranging from 500 to 1,600 nm.

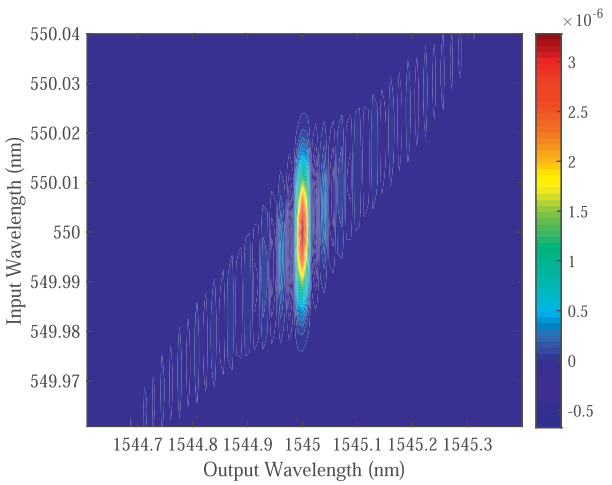

FIGURE 5 | Simulated transfer function when the pump bandwidth $\delta\omega_p$ is 50 GHz.

niobate (LN), respectively. The LN layer is made from X-cut LNOI film and the waveguide propagates in y-direction with a sidewall angle of $\varphi = 60^{\circ}$, and a length of $L = 10$ mm. The waveguide height h and its bottom ridge width w restrict the transverse distribution of the guide mode and can be adjusted in structure design and fabrication process. By varying the height and width, light dispersion can be tuned in the LNOI waveguide. In order to characteristic the property of the bandwidth compressor, numerically simulations of group index and effective refractive index are obtained by utilizing the Mode Solution software with the material dispersion of LN given by Ref. [35].

Here we aim to design a counter-propagating DFG process that converts the broadband input photons centered at 550 nm in TE_{00} mode to narrowband output photons centered at 1,545 nm in TM_{00} mode with a pulsed laser light centered at 854 nm in TM_{00} mode as the pump. Such frequency conversion process with the chosen wavelengths may connect the quantum communication channels with single-photon emitters around 550 nm, such as the charge-neutral nitrogen-vacancy center in diamond [36] and the CdSe quantum dots [37, 38]. The structure parameters are $h = 0.6$ μm and $w = 0.8$ μm. Single mode condition can be achieved at 1,545 nm with the field distribution of TE_{00} and TE_{00} modes shown in **Figure 3**. With simulated effective index of the waveguide, we can calculate the poling period to be $\Lambda = 0.402$ μm for satisfying the first-order QPM condition of $\Delta k = 0$ according to **Eq. 5**. The simulated results of group index $n_g = c/u$ of TE_{00} and TM_{00} modes with wavelength ranging from 500 to 1,600 nm are shown in **Figure 4**. Explicitly, the simulated group indexes of the pump light at 854 nm in TM_{00} mode, the input light at 550 nm in TE_{00} mode, and the output light at 1,545 nm in TM_{00} mode are $n_{g,p} = 2.533$, $n_{g,i} = 2.532$, and $n_{g,o} = 2.401$, respectively. Therefore, we can obtain $\delta\omega_1 = 60$ THz and $\delta\omega_2 = 12.2$ GHz.

In order to show the spectrum relation between the input and output photons, we simulate the transfer function given by **Eq. 10**. By assuming a Gaussian spectrum pump, the simulation

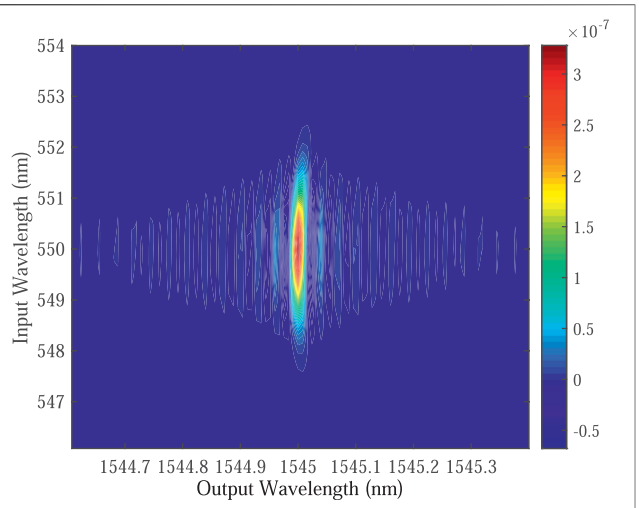

FIGURE 6 | Simulated transfer function when the pump bandwidth $\delta\omega_p$ is 5 THz.

results when pump bandwidths $\delta\omega_p$ = 50 GHz and $\delta\omega_p$ = 5 THz are shown in **Figure 5**, **6**, respectively. The corresponding Schmidt numbers K are estimated to be 1.037, and 1.041, respectively. Hence, we can see that the transfer function is very close to a separable one. The bandwidth of the output photon can be estimated from **Eq. 17**, namely, $\delta\omega_o$ = 33 GHz. Then according to **Eq. 18** we can express the bandwidth compression factor as

$$\eta = \frac{\delta\omega_i}{\delta\omega_o} = \frac{\delta\omega_p}{33\ \text{GHz}}, \tag{19}$$

and consequently, in our simulation range of $\delta\omega_p$ = 50 GHz ~ 5 THz, we can obtain a compression factor ranging from 1.5 to 150.

Then we give a simulation of the conversion efficiency. The DFG process with a separable transfer function can be treated as a BS model and the conversion efficiency is given by $sin^2\theta$ [31]. Here the coupling parameter can be expressed as

$$\theta = \frac{2d\pi^2 LN}{c}\sqrt{\frac{2P_p\omega_{i0}\omega_{o0}}{c\varepsilon_0 n_{p0}n_{i0}n_{o0}\left|\int d\omega_p \alpha(\omega_p)\right|^2 B}}, \tag{20}$$

where $d = 2d_{31}/(m\pi)$ is the nonlinear coefficient, and P_p is the pump peak power, with n_j ($j = p, i, o$) representing the effective refractive index of pump, input and output lights at central frequencies, respectively. The parameter N is the normalization factor of transfer function given by

$$N = \sqrt{\int d\omega_i d\omega_o |f(\omega_i, \omega_o)|^2}. \tag{21}$$

The effective interaction area B can be written as

$$B = \left[\int dxdz g_p(x,z) g_i(x,z) g_o^*(x,z)\right]^{-2}, \tag{22}$$

where $g_j(x, z)$ ($j = p, i, o$) is the normalized spatial distribution of the cross-sectional area of pump, input and output fields, respectively. Through numerical simulation using the Mode solution software, we estimated B to be 0.472 μm^2. With these calculations, we can estimate a pump peak power of 2.04 W in the case of unity conversion efficiency. If setting the pump pulse width to be 200 fs with a repetition rate of 80 MHz, we can calculate the average pump power to be 0.032 mW, which is much lower than the previous experiment results [39, 40].

It should be noted that the ideal unity conversion efficiency in a single process could be achieved only in the limit of short interaction length or long pump pulse [41]. In broadband mode case, time-ordering corrections may affect the conversion efficiency [42, 43], which are resulted from the noncommutativity of the interaction Hamiltonian at different times. A maximum conversion efficiency of 87.7% has been obtained in a SFG process [44]. Moreover, Reddy *et al.* [45] proposed a scheme to overcome the time-ordering correction limitation by cascading two frequency conversion processes with 50% conversion efficiency.

4 DISCUSSION

We would like to discuss the experimental feasibility of our design. The LNOI waveguide structure is experimentally feasible with current LNOI fabrication techniques [27–30]. The poling period on the order of 0.402 μm is still challenging at present. However, we can use a higher-order reciprocal wave vector to obtain a bigger poling period at the cost of lower efficiency. For example, if using the third-order reciprocal wave vector, we would get a poling period of 1.206 μm with the nonlinear coefficient reduced to $d/3$. Such poling period is possible with current fabrication techniques [46].

In conclusion, we proposed a scheme to realize optical frequency down-conversion and bandwidth compression via the counter-propagating QPM DFG process, which can provide a quantum network interface for devices working at different central frequencies and bandwidths. We proved that, due to the counter-propagation configuration, a separable spectrum transfer function can be obtained only by choosing the pump bandwidth in a range between two characteristic bandwidth scales, rather than satisfying constrained dispersion and group velocity relations, and thus this method is not strictly limited by the material, dispersion, and working wavelength. Moreover, under this condition, the input photon can have a bandwidth the same with that of the pump light, while the bandwidth of the out photon is only determined by the phase-matching function irrespective of the pump bandwidth. Such feature enables a large bandwidth compression factor as well as facilitates the application in the interface between photons with different spectral shapes. We designed a periodically-poled LNOI waveguide to realize the scheme. The simulation result shows a nearly separable transfer function with the Schmidt number estimated very close to 1. By changing the pump bandwidth, a bandwidth compression factor ranging from 1.5 to 150 can be obtained. We also calculate a pump

average power of 0.032 mW to achieve unit conversion efficiency. In addition, the counter-propagating output feature is also of great benefit to compressing co-propagating noises. Finally, our approach opens up a way for efficient optical interface connecting photons with different frequency and spectrum bandwidth benefiting from the counter-propagating nonlinear process. We hope our approach can stimulate more such investigations.

DATA AVAILABILITY STATEMENT

The original contributions presented in the study are included in the article/Supplementary Material, further inquiries can be directed to the corresponding authors.

AUTHOR CONTRIBUTIONS

D-JG designed the scheme and performed the calculations with the help of RY. Y-XG, and ZX supervised the project. All authors discussed the results and reviewed the manuscript.

FUNDING

This work was supported by the National Key R&D Program of China (No. 2019YFA0705000), Key R&D Program of Guangdong Province (No. 2018B030329001), Leading-edge technology Program of Jiangsu Natural Science Foundation (No. BK20192001), National Natural Science Foundation of China (51890861, 11690031, 11674169, 11974178).

REFERENCES

1. Duan L-M, Lukin MD, Cirac JI, and Zoller P. Long-distance Quantum Communication With Atomic Ensembles and Linear Optics. *Nature* (2001) 414:413–8. doi:10.1038/35106500
2. Boaron A, Boso G, Rusca D, Vulliez C, Autebert C, Caloz M, et al. Secure Quantum Key Distribution Over 421 Km of Optical Fiber. *Phys Rev Lett* (2018) 121:190502. doi:10.1103/PhysRevLett.121.190502
3. Knill E, Laflamme R, and Milburn GJ. A Scheme for Efficient Quantum Computation With Linear Optics. *nature* (2001) 409:46–52. doi:10.1038/35051009
4. Kok P, Munro WJ, Nemoto K, Ralph TC, Dowling JP, and Milburn GJ. Linear Optical Quantum Computing With Photonic Qubits. *Rev Mod Phys* (2007) 79: 135–74. doi:10.1103/RevModPhys.79.135
5. Lvovsky AI, Sanders BC, and Tittel W. Optical Quantum Memory. *Nat Photon* (2009) 3:706–14. doi:10.1038/nphoton.2009.231
6. Kozhekin AE, Mølmer K, and Polzik E. Quantum Memory for Light. *Phys Rev A* (2000) 62:033809. doi:10.1103/PhysRevA.62.033809
7. Karpiński M, Jachura M, Wright LJ, and Smith BJ. Bandwidth Manipulation of Quantum Light by an Electro-Optic Time Lens. *Nat Photon* (2017) 11:53–7. doi:10.1038/nphoton.2016.228
8. Wright LJ, Karpiński M, Söller C, and Smith BJ. Spectral Shearing of Quantum Light Pulses by Electro-Optic Phase Modulation. *Phys Rev Lett* (2017) 118: 023601. doi:10.1103/PhysRevLett.118.023601
9. Sośnicki F, and Karpiński M. Large-Scale Spectral Bandwidth Compression by Complex Electro-Optic Temporal Phase Modulation. *Opt Express* (2018) 26: 31307–16. doi:10.1364/OE.26.031307
10. Vandevender AP, and Kwiat PG. High Efficiency Single Photon Detection *via* Frequency Up-Conversion. *J Mod Opt* (2004) 51:1433–45. doi:10.1080/09500340408235283
11. Albota MA, and Wong FNC. Efficient Single-Photon Counting at 155 Mm by Means of Frequency Upconversion. *Opt Lett* (2004) 29:1449–51. doi:10.1364/ol.29.001449
12. Kobayashi T, Ikuta R, Yasui S, Miki S, Yamashita T, Terai H, et al. Frequency-Domain Hong-Ou-Mandel Interference. *Nat Photon* (2016) 10:441–4. doi:10.1038/nphoton.2016.74
13. Ikuta R, Kobayashi T, Yasui S, Miki S, Yamashita T, Terai H, et al. Frequency Down-Conversion of 637 Nm Light to the Telecommunication Band for Non-Classical Light Emitted From Nv Centers in diamond. *Opt Express* (2014) 22: 11205–14. doi:10.1364/OE.22.011205
14. Vollmer CE, Baune C, Samblowski A, Eberle T, Händchen V, Fiurášek J, et al. Quantum Up-Conversion of Squeezed Vacuum States from 1550 to 532 Nm. *Phys Rev Lett* (2014) 112:073602. doi:10.1103/PhysRevLett.112.073602
15. Rakher MT, Ma L, Slattery O, Tang X, and Srinivasan K. Quantum Transduction of Telecommunications-Band Single Photons From a Quantum Dot by Frequency Upconversion. *Nat Photon* (2010) 4:786–91. doi:10.1038/nphoton.2010.221
16. Walker T, Miyanishi K, Ikuta R, Takahashi H, Vartabi Kashanian S, Tsujimoto Y, et al. Long-Distance Single Photon Transmission From a Trapped Ion via Quantum Frequency Conversion. *Phys Rev Lett* (2018) 120:203601. doi:10.1103/physrevlett.120.203601
17. Lavoie J, Donohue JM, Wright LG, Fedrizzi A, and Resch KJ. Spectral Compression of Single Photons. *Nat Photon* (2013) 7:363–6. doi:10.1038/nphoton.2013.47
18. Allgaier M, Ansari V, Sansoni L, Eigner C, Quiring V, Ricken R, et al. Highly Efficient Frequency Conversion With Bandwidth Compression of Quantum Light. *Nat Commun* (2017) 8:1–6. doi:10.1038/ncomms14288
19. Harris SE. Proposed Backward Wave Oscillation in the Infrared. *Appl Phys Lett* (1966) 9:114–6. doi:10.1063/1.1754668
20. Gatti A, Corti T, and Brambilla E. Temporal Coherence and Correlation of Counterpropagating Twin Photons. *Phys Rev A* (2015) 92:053809. doi:10.1103/physreva.92.053809
21. Gong YX, Xie ZD, Xu P, Yu XQ, Xue P, and Zhu SN. Compact Source of Narrow-Band Counterpropagating Polarization-Entangled Photon Pairs Using a Single Dual-Periodically-Poled Crystal. *Phys Rev A* (2011) 84: 053825. doi:10.1103/physreva.84.053825
22. Duan J-C, Zhang J-N, Zhu Y-J, Sun C-W, Liu Y-C, Xu P, et al. Generation of Narrowband Counterpropagating Polarization-Entangled Photon Pairs Based on Thin-Film Lithium Niobate on Insulator. *J Opt Soc Am B* (2020) 37: 2139–45. doi:10.1364/josab.395108
23. Christ A, Eckstein A, Mosley PJ, and Silberhorn C. Pure Single Photon Generation by Type-I Pdc With Backward-Wave Amplification. *Opt Express* (2009) 17:3441–6. doi:10.1364/OE.17.003441
24. Luo K-H, Ansari V, Massaro M, Santandrea M, Eigner C, Ricken R, et al. Counter-Propagating Photon Pair Generation in a Nonlinear Waveguide. *Opt Express* (2020) 28:3215–25. doi:10.1364/OE.378789
25. Cai W-H, Wei B, Wang S, and Jin R-B. Counter-propagating Spectrally Uncorrelated Biphotons at 1550 Nm Generated From Periodically Poled MTiOXO4 (M = K, Rb, Cs; X = P, as). *J Opt Soc Am B* (2020) 37:3048–54. doi:10.1364/JOSAB.401157
26. Liu Y-C, Guo D-J, Ren K-Q, Yang R, Shang M, Zhou W, et al. Observation of Frequency-Uncorrelated Photon Pairs Generated by Counter-propagating Spontaneous Parametric Down-Conversion. *Sci Rep* (2021) 11:1–6. doi:10.1038/s41598-021-92141-y
27. Boes A, Corcoran B, Chang L, Bowers J, and Mitchell A. Status and Potential of Lithium Niobate on Insulator (Lnoi) for Photonic Integrated Circuits. *Laser Photon Rev* (2018) 12:1700256. doi:10.1002/lpor.201700256
28. Wang C, Langrock C, Marandi A, Jankowski M, Zhang M, Desiatov B, et al. Ultrahigh-Efficiency Wavelength Conversion in Nanophotonic Periodically Poled Lithium Niobate Waveguides. *Optica* (2018) 5:1438–41. doi:10.1364/optica.5.001438
29. Chen J-Y, Ma Z-H, Sua YM, Li Z, Tang C, and Huang Y-P. Ultra-Efficient Frequency Conversion in Quasi-Phase-Matched Lithium Niobate Microrings. *Optica* (2019) 6:1244–5. doi:10.1364/OPTICA.6.001244

30. Lu J, Surya JB, Liu X, Bruch AW, Gong Z, Xu Y, et al. Periodically Poled Thin-Film Lithium Niobate Microring Resonators With a Second-Harmonic Generation Efficiency of 250,000%/w. *Optica* (2019) 6:1455–60. doi:10.1364/OPTICA.6.001455
31. Eckstein A, Brecht B, and Silberhorn C. A Quantum Pulse Gate Based on Spectrally Engineered Sum Frequency Generation. *Opt Express* (2011) 19: 13770–8. doi:10.1364/OE.19.013770
32. Law CK, Walmsley IA, and Eberly JH. Continuous Frequency Entanglement: Effective Finite hilbert Space and Entropy Control. *Phys Rev Lett* (2000) 84: 5304–7. doi:10.1103/PhysRevLett.84.5304
33. Prasad S, Scully MO, and Martienssen W. A Quantum Description of the Beam Splitter. *Opt Commun* (1987) 62:139–45. doi:10.1016/0030-4018(87)90015-0
34. Baronavski AP, Ladouceur HD, and Shaw JK. Analysis of Cross Correlation, Phase Velocity Mismatch and Group Velocity Mismatches in Sum-Frequency Generation. *IEEE J Quan Electron.* (1993) 29:580–9. doi:10.1109/3.199312
35. Zelmon DE, Small DL, and Jundt D. Infrared Corrected Sellmeier Coefficients for Congruently Grown Lithium Niobate and 5 mol.% Magnesium Oxide–Doped Lithium Niobate. *JOSA B* (1997) 14:3319–22. doi:10.1364/JOSAB.14.003319
36. Aharonovich I, Castelletto S, Simpson DA, Su C-H, Greentree AD, and Prawer S. Diamond-Based Single-Photon Emitters. *Rep Prog Phys* (2011) 74:076501. doi:10.1088/0034-4885/74/7/076501
37. Chen O, Zhao J, Chauhan VP, Cui J, Wong C, Harris DK, et al. Compact High-Quality CdSe-CdS Core-Shell Nanocrystals With Narrow Emission Linewidths and Suppressed Blinking. *Nat Mater* (2013) 12:445–51. doi:10.1038/nmat3539
38. Lin X, Dai X, Pu C, Deng Y, Niu Y, Tong L, et al. Electrically-Driven Single-Photon Sources Based on Colloidal Quantum Dots With Near-Optimal Antibunching at Room Temperature. *Nat Commun* (2017) 8:1132–7. doi:10.1038/s41467-017-01379-6
39. Tanzilli S, Tittel W, Halder M, Alibart O, Baldi P, Gisin N, et al. A Photonic Quantum Information Interface. *Nature* (2005) 437:116–20. doi:10.1038/nature04009
40. Roussev RV, Langrock C, Kurz JR, and Fejer MM. Periodically Poled Lithium Niobate Waveguide Sum-Frequency Generator for Efficient Single-Photon Detection at Communication Wavelengths. *Opt Lett* (2004) 29:1518–20. doi:10.1364/OL.29.001518
41. Donohue JM, Mazurek MD, and Resch KJ. Theory of High-Efficiency Sum-Frequency Generation for Single-Photon Waveform Conversion. *Phys Rev A* (2015) 91:033809. doi:10.1103/PhysRevA.91.033809
42. Christ A, Brecht B, Mauerer W, and Silberhorn C. Theory of Quantum Frequency Conversion and Type-Ii Parametric Down-Conversion in the High-Gain Regime. *New J Phys* (2013) 15:053038. doi:10.1088/1367-2630/15/5/053038
43. Quesada N, and Sipe JE. High Efficiency in Mode-Selective Frequency Conversion. *Opt Lett* (2016) 41:364–7. doi:10.1364/ol.41.000364
44. Brecht B, Eckstein A, Ricken R, Quiring V, Suche H, Sansoni L, et al. Demonstration of Coherent Time-Frequency Schmidt Mode Selection Using Dispersion-Engineered Frequency Conversion. *Phys Rev A* (2014) 90: 030302. doi:10.1103/physreva.90.030302
45. Reddy DV, Raymer MG, and McKinstrie CJ. Efficient Sorting of Quantum-Optical Wave Packets by Temporal-Mode Interferometry. *Opt Lett* (2014) 39: 2924–7. doi:10.1364/ol.39.002924
46. Younesi M, Kumar P, Stanicki BJ, Geiss R, Chang WK, and Chen YH. Periodic Poling With Short Period for Thin Film Lithium Niobate Waveguides. In: Lasers and Electro-Optics Europe & European Quantum Electronics Conference (2019) IEEE. doi:10.1109/cleoe-eqec.2019.8871472

Conflict of Interest: The authors declare that the research was conducted in the absence of any commercial or financial relationships that could be construed as a potential conflict of interest.

Publisher's Note: All claims expressed in this article are solely those of the authors and do not necessarily represent those of their affiliated organizations, or those of the publisher, the editors and the reviewers. Any product that may be evaluated in this article, or claim that may be made by its manufacturer, is not guaranteed or endorsed by the publisher.